

## Wetting of grain boundaries in Al by the solid $\text{Al}_3\text{Mg}_2$ phase

B. B. Straumal · B. Baretzky · O. A. Kogtenkova ·  
A. B. Straumal · A. S. Sidorenko

Received: 1 May 2009 / Accepted: 31 October 2009 / Published online: 12 November 2009  
© The Author(s) 2009. This article is published with open access at Springerlink.com

**Abstract** The microstructure of binary  $\text{Al}_{100-x}\text{Mg}_x$  ( $x = 10, 15, 18$  and  $25$  wt%) alloys after long anneals (600–4000 h) was studied between 210 and 440 °C. The transition from incomplete to complete wetting of Al/Al grain boundaries (GBs) by the second solid phase  $\text{Al}_3\text{Mg}_2$  has been observed. The portion of completely wetted GBs increases with increasing temperature beginning from  $T_{\text{wsmin}} = 220$  °C. Above  $T_{\text{wsmax}} = 410$  °C all Al/Al GBs are completely wetted by the  $\text{Al}_3\text{Mg}_2$  phase.

### Introduction

The equilibrium and reversible transition from incomplete to complete wetting of grain boundaries (GBs) by the liquid phase (melt) has been experimentally observed in a number of systems like Zn–Sn, Ag–Pb, Al–Cd, Al–In, Al–Pb, W–Ni, W–Cu, W–Fe, Mo–Ni, Mo–Cu, Mo–Fe, Cu–In, Al–Sn [1–6]. The formation of continuous layers of a liquid phase between solid grains is broadly used, particularly in

welding, soldering and liquid-phase sintering. Recently, this has been observed in the Zn–Al alloys that similar GB wetting transition can proceed even in case when a second phase wetting GBs is solid [7]. There are good reasons to expect that the complete wetting of GBs by a second solid phase can be observed in many technologically important systems. Especially “suspicious” are the alloys where the complete GB wetting by a melt was already observed, like for example the Al–Mg alloys [8]. The Al–Mg system forms a base of the important class of Al alloys. The eventual formation of equilibrium GB layers of a rather brittle  $\text{Al}_3\text{Mg}_2$  phase can drastically influence the mechanical properties of the Al–Mg alloys. Therefore, the search for the conditions where the Al/Al GBs could be completely wetted by the second solid phase  $\text{Al}_3\text{Mg}_2$  is very important.

### Experimental

The Al–Mg alloys with 10, 15, 18 and 25 wt% Mg (Fig. 1) were prepared from the high-purity 5N Al and 4N5 Mg by a vacuum induction melting in a form of cylindrical ingots. The 2 mm thick slices were cut from the  $\varnothing$  20 mm cylindrical Al–Mg ingots, each slice was cut into four segments, and each sample was sealed into evacuated silica ampoule with a residual pressure of approximately  $4 \times 10^{-4}$  Pa at room temperature. Samples were annealed at temperatures between 210 and 440 °C (see experimental points in the Al–Mg phase diagram, Fig. 1) during long time (between 4000 h at 210 °C and 600 h at 440 °C), and then quenched in water. The accuracy of the annealing temperature was  $\pm 2$  °C. After quenching, samples were embedded in resin and then mechanically ground and polished, using 1  $\mu\text{m}$  diamond paste in the last polishing

---

B. B. Straumal (✉) · O. A. Kogtenkova · A. B. Straumal  
Institute of Solid State Physics Russian Academy of Sciences,  
142432 Chernogolovka, Russia  
e-mail: straumal@issp.ac.ru; straumal@mf.mpg.de

B. B. Straumal · B. Baretzky  
Max-Planck Institut für Metallforschung, Heisenbergstraße 3,  
70569 Stuttgart, Germany

A. B. Straumal  
Moscow State Institute of Steel and Alloys (Technological  
University), Leninsky prospect 4, 119991 Moscow, Russia

A. S. Sidorenko  
Institute of Applied Physics, LISES AS RM, Academiei 5,  
Kishinev, MD 2028, Moldova

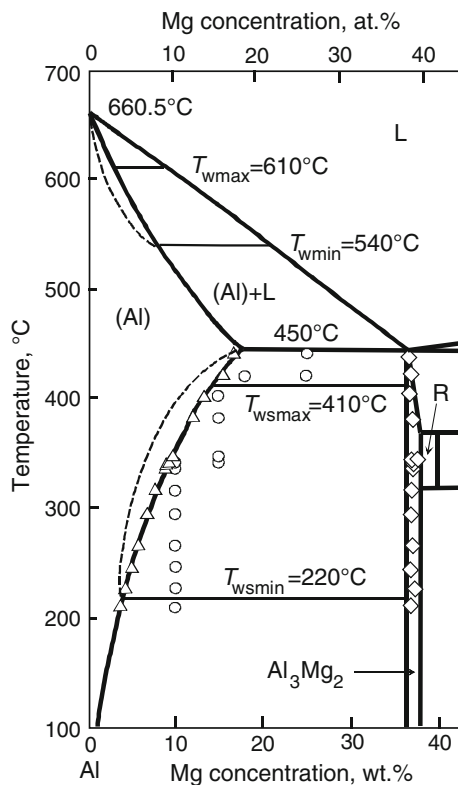


**Fig. 1** Part of the Al–Mg phase diagram. *Thick lines* denote the bulk phase transitions and are taken from Ref. [9]. *Thin horizontal lines* are the tie-lines of GB wetting phase transitions.  $T_{wmax}$  and  $T_{wmin}$  for the GB wetting by a liquid phase are taken from Ref. [8].  $T_{wsmax}$  and  $T_{wsmin}$  for the GB wetting by a second solid phase  $Al_3Mg_2$  were determined in the present work. *Circles* denote the points where the wetting annealings were performed. *Triangles* denote the measured concentration in the (Al) solid solution. *Diamonds* denote the measured concentration in the  $Al_3Mg_2$  solid phase. *Dotted lines* denote the hypothetical GB solidus and solvus

step, for the metallographic study. After etching, samples were investigated by means of the light microscopy and scanning electron microscopy (SEM). SEM investigations were carried out in a Tescan Vega TS5130 MM microscope equipped by the LINK energy-dispersive spectrometer produced by Oxford Instruments. Using the same equipment, the composition of various structural elements in the annealed and quenched samples was controlled with the aid of electron probe microanalysis. Light microscopy has been performed using Neophot-32 light microscope equipped with 10 Mpix Canon Digital Rebel XT camera. A quantitative analysis of the wetting transition was performed adopting the following criterion: every Al/Al GB was considered to be completely wetted only when a layer of  $Al_3Mg_2$  had covered the whole GB; if such a layer appeared to be interrupted, the GB was regarded as a partially wetted. At least 100 GBs were analysed at each temperature. Typical micrographs obtained by SEM are shown in Fig. 2.

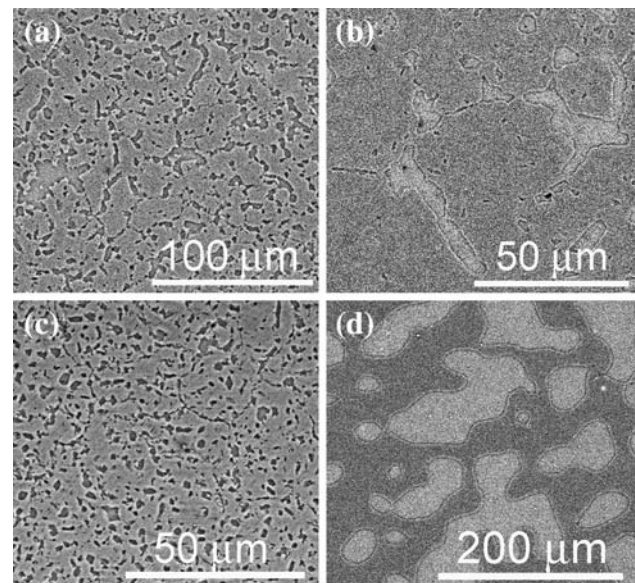


**Fig. 2** SEM micrographs of Al–Mg alloys: **a** Al–10 wt% Mg alloy annealed at 210 °C, 4000 h; **b** Al–10 wt% Mg alloy annealed at 225 °C, 3600 h; **c** Al–10 wt% Mg alloy annealed at 335 °C, 2180 h; **d** Al–18 wt% Mg alloy annealed at 420 °C, 600 h. The Al-based solid solution grains appear *light grey*, the  $Al_3Mg_2$  phase appears *dark grey* in all micrographs

## Results and discussion

SEM micrograph of the Al–10 wt% Mg alloy annealed at 210 °C, 4000 h is shown in Fig. 2a. The particles of the  $Al_3Mg_2$  phase (appears dark grey) form chains along Al/Al GBs. The grains of the Al-based solid solution appear light grey. It has to be underlined that the Al/ $Al_3Mg_2$  interphase boundaries (IBs) are not smooth (like for example the Al/Zn interphase boundaries in the Al–Zn alloys are [7, 26, 27]). Most probably it is due to the strong anisotropy of the interfacial energy of Al/ $Al_3Mg_2$  IBs. No Al/Al GBs completely wetted by the layers of the  $Al_3Mg_2$  phase are visible. The contact angles between  $Al_3Mg_2$  particles and Al/Al GBs are small, but not zero. The microstructure of the Al–10 wt% Mg alloy annealed at 225 °C, 3600 h is shown in Fig. 2b. First Al/Al GBs completely wetted by the continuous layers of the  $Al_3Mg_2$  phase appear. Therefore, the temperature of the beginning of GB wetting transition is  $T_{wsmin} = 220$  °C. With increasing temperature the portion of the Al/Al GBs completely wetted by the  $Al_3Mg_2$  phase increases (see for example the micrograph of the Al–10 wt% Mg alloy annealed at 335 °C, 2180 h, Fig. 2c). Unfortunately, the Al/ $Al_3Mg_2$  IBs are not smooth. It makes complicated the calculation of the portion of completely wetted GBs. Therefore, in order to distinguish between completely and incompletely wetted GBs we used the criterion from the Cahn’s work [12]: “If the minor phase wets GBs, the major phase is distributed as droplets in the

minor phase”. Above the maximal temperature of the GB wetting transition  $T_{w\max} = 410\text{ }^\circ\text{C}$  all Al/Al GBs are completely wetted by the  $\text{Al}_3\text{Mg}_2$  phase and separated from each other by the continuous  $\text{Al}_3\text{Mg}_2$  layers (see as example the micrograph of the Al–18 wt% Mg alloy annealed at  $420\text{ }^\circ\text{C}$ , 600 h, Fig. 2d). It is visible in Fig. 2d that the Al/ $\text{Al}_3\text{Mg}_2$  IBs remain faceted at  $420\text{ }^\circ\text{C}$ , though they are slightly smoother than at lower temperatures. The thickness of the  $\text{Al}_3\text{Mg}_2$  wetting layers depends on the amount of phase. Generally, it increases with increasing Mg content in the alloys. Therefore, we used the Al–Mg alloys with various Mg content in order to keep minimal the amount of  $\text{Al}_3\text{Mg}_2$  phase at each annealing temperature (see Fig. 1) in order to distinguish the complete and incomplete GB wetting. Our goal was to prevent as long as possible the merging of  $\text{Al}_3\text{Mg}_2$  particles into a continuous layer. The fraction of wetted GBs in the Al–Mg polycrystals is shown as a function of the temperature in Fig. 3. Different symbols correspond to the different compositions of studied Al–Mg alloys. Between  $T_{w\min} = 220\text{ }^\circ\text{C}$  and  $T_{w\max} = 410\text{ }^\circ\text{C}$  the fraction of the wetted GBs gradually increases with increasing temperature from 0 to 100%.

Thin equilibrium GB or surface films were first considered by Cahn [10] and Ebner and Saam [11]. They proposed the idea that the transition from incomplete to complete surface wetting is a phase transformation. Cahn also analysed the case when wetting phase is solid [12]. Later the idea of wetting transformations was successfully applied for GBs, also old data on GB wetting were reconsidered from this point of view [3–6]. The phenomenon of the transition from incomplete to complete wetting is more general than the wetting under the consolute point

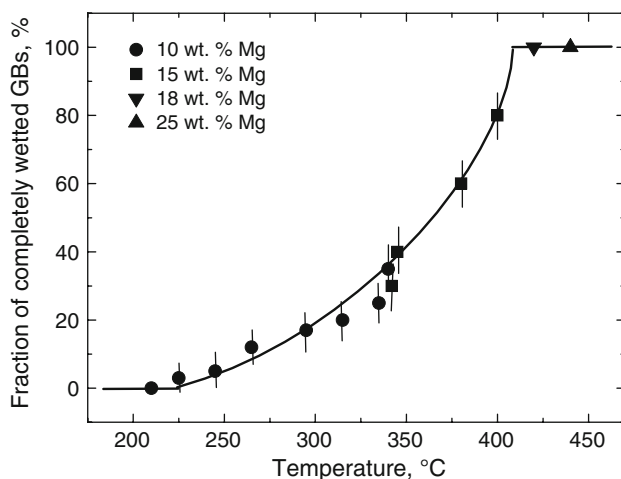


**Fig. 3** Temperature dependence for the fraction of Al/Al GBs completely wetted by the  $\text{Al}_3\text{Mg}_2$  phase. Different symbols correspond to the different compositions of studied Al–Mg alloys: circles 10 wt% Mg, squares 15 wt% Mg, inverted triangle 18 wt% Mg, upright triangle 25 wt% Mg

originally proposed by Cahn [10, 12] and analysed further in numerous works [13, 14]. The modified Cahn’s model was developed based on the numerous experimental results [15]. The transition from incomplete to complete wetting occurs in all systems where the temperature dependences of interface energies intersect [15]. In particular GB wetting phase transformation proceeds at the temperature  $T_w$  where GB energy  $\sigma_{\text{GB}}$  becomes equal to the energy  $2\sigma_{\text{SL}}$  of two solid/liquid interfaces. Above  $T_w$  GB is substituted by a layer of the melt. The tie-line of the GB wetting phase transition appears in the two-phase area of a bulk phase diagram. For example, in the (Al) + L two-phase region of the Al–Mg system the GB transformation for the Al/Al GBs wetting by Mg-containing melt occurs [8]. The completely wetted GBs in the Al–Mg polycrystals do not exist below  $T_{w\min} = 540\text{ }^\circ\text{C}$ .  $T_{w\min}$  is the wetting temperature for a GB with maximal energy  $\sigma_{\text{GBmax}}$ . Above  $T_{w\max} = 610\text{ }^\circ\text{C}$  all high-angle GBs in (Al) are completely wetted by the melt [8].  $T_{w\max}$  is the wetting temperature for a GB with minimal energy  $\sigma_{\text{GBmin}}$ . Between  $T_{w\min}$  and  $T_{w\max}$  the wetting tie-lines for GBs with intermediate  $\sigma_{\text{GBmax}} > \sigma_{\text{GB}} > \sigma_{\text{GBmin}}$  are positioned in the (Al) + L area (Fig. 1). GBs can also be “wetted” by a second solid phase, as we can see in the present work, too [12, 14]. The reversible transition from incomplete to complete solid phase wetting was observed for the first time in the Zn–Al system [7].

Following the Cahn’s generic phase diagram, the more sophisticated theories of GB phases, segregation and wetting layers were developed [13–15]. Thin films of interfacial phases were observed in GBs in metals (works of Luo and coworkers [16, 36, 37]), in oxides ([17], see also concept of complexions by Harmer et al. [18–22]), in interphase boundaries (Kaplan and coworkers [23–25]). According to those developments the GB wetting tie-lines continue as prewetting (or GB solidus or solvus) lines in the one-phase (Al) area. Such GB solidus and/or solvus lines should exist also in the Al–Mg system. Just one GB solidus line for  $T_{w\min}$  and one GB solvus line for  $T_{w\min}$  is shown for simplicity in Fig. 1. The experimental evidence for the existence of a GB liquid-like phase between GB solidus line and bulk solidus line was obtained by transmission electron microscopy (TEM) [26] and differential scanning calorimetry (DSC) for the Al–Zn alloys [27]. In the area between GB solidus and bulk solidus, GB contains the thin layer of a GB phase. The energy gain ( $\sigma_{\text{GB}} - 2\sigma_{\text{SL}}$ ) above  $T_{w\text{GB}}$  permits to stabilise such thin layer of a GB phase between the abutting crystals, which is metastable in the bulk and become stable in the GB. The formation of metastable phase layer of thickness  $l$  leads to the energy loss  $l\Delta g$ . ( $\Delta g$  being the additional energy needed to produce the thermodynamically metastable liquid phase). Finite thickness  $l$  of the GB phase is defined by the equality of the energy gain ( $\sigma_{\text{GB}} - 2\sigma_{\text{SL}}$ ) and energy loss  $l\Delta g$ . In this

simplest model, the prewetting GB layer of finite thickness  $l$  suddenly appears by crossing the prewetting (GB solidus) line  $c_{bt}(T)$ . Thickness  $l$  logarithmically diverges close to the bulk solidus. It comes about from an assumption that the size of the system is infinite. Moreover, the thickness of a wetting phase is thermodynamically infinite in the two-phase area. Physically, in the two-phase area, its thickness is defined only by the amount of the wetting phase. Several monolayer (ML) thick liquid-like GB layers possessing high diffusivity were observed in the Cu–Bi [28–31], Al–Zn [26, 27], Fe–Si–Zn [32–35] and W–Ni alloys [36, 37]. GB liquid-like phase drastically influences also the GB segregation [29], GB mobility [38], GB energy and electrical resistivity [39, 40]. The direct HREM evidence for thin GB films and triple junction “pockets” has been recently obtained in metallic W–Ni [36, 37] and Al–Zn [26] alloys.

The observed splitting of the solidus line into conventional bulk solidus and novel GB solidus permitted explaining the mysterious phenomenon of the high strain-rate superplasticity (HSRS) observed in several nanostructured Al ternary alloys and nanostructured Al metal-matrix composites, containing Mg and Zn [41–47]. The maximal elongation-to-failure increased drastically from 200–300% upto 2000–2500% in a very narrow temperature interval of about 10 °C just below the respective solidus temperature. Very long time no satisfactory explanation was offered for this phenomenon. In Refs. [26, 27], we explained the extremely high plasticity in the Al-based alloys by the presence of thin liquid-like layers of the thermodynamically stable GB phase close to the bulk solidus line. Is it possible to explain the high plasticity in the Al-based alloys at room temperature using similar wetting phenomena?

In summary, the GB wetting phase transition proceeds in the Al-rich alloys in the Al–Mg system. The new GB tie-lines appear in the Al–Mg phase diagram (Fig. 1). Below the tie-line at  $T_{wsmin} = 220$  °C no Al/Al GBs wetted by the second solid phase  $Al_3Mg_2$  are present in the polycrystals. Above the tie-line at  $T_{wsmax} = 410$  °C all Al/Al GBs are wetted by the second solid phase and separated from each other by the continuous  $Al_3Mg_2$  layers. This phenomenon can be used for the tailoring of mechanical properties of the Mg-doped Al alloys. The novel information on GB wetting tie-lines will be used for the search of thin GB phases above  $T_{wsmin}$  close to the bulk solvus line in the Al–Mg system.

**Acknowledgements** Authors thank the Russian Foundation for Basic Research (contracts 08-08-90105 and 08-08-91302) and the Academy of Sciences of Moldova (Grant 43/R) for the financial support. Authors cordially thank Prof. E. Rabkin, Prof. R. Valiev and Dr. S. Protasova for stimulating discussions, Mr. A. Nekrasov for the help with SEM and EPMA measurements.

**Open Access** This article is distributed under the terms of the Creative Commons Attribution Noncommercial License which permits any noncommercial use, distribution, and reproduction in any medium, provided the original author(s) and source are credited.

## References

1. Passerone A, Eustathopoulos N, Desré P (1977) *J Less-Common Met* 52:37
2. Passerone A, Sangiorgi R, Eustathopoulos N (1982) *Scripta Metall* 16:547
3. Eustathopoulos N (1983) *Int Met Rev* 28:189
4. Straumal BB (2003) Grain boundary phase transitions. Nauka Publishers, Moscow (in Russian)
5. Straumal B, Muschik T, Gust W, Predel B (1992) *Acta Metall Mater* 40:939
6. Straumal B, Molodov D, Gust W (1995) *Interface Sci* 3:127
7. López GA, Mittemeijer EJ, Straumal BB (2004) *Acta Mater* 52:4537
8. Straumal BB, López G, Mittemeijer EJ et al (2003) *Def Diff Forum* 216:307
9. Massalski TB (ed) (1990) Binary alloy phase diagrams, 2nd edn. ASM International, Materials Park
10. Cahn JW (1977) *J Chem Phys* 66:3667
11. Ebner C, Saam WF (1977) *Phys Rev Lett* 38:1486
12. Cahn JW (2000) *Phys A* 279:195
13. Wynblatt P, Saul A, Chatain D (1998) *Acta Mater* 46:2337
14. Wynblatt P, Chatain D (2008) *Mater Sci Eng A* 495:119
15. Bishop CM, Tang M, Cannon RM, Carter WC (2006) *Mater Sci Eng A* 422:102
16. Luo J (2008) *Curr Opin Sol State Mater Sci* 12:81
17. Luo J, Chiang Y-M (2008) *Ann Rev Mater Res* 38:227
18. Luo J, Dillon SJ, Harmer MP (2009) *Micros Today* 17:22
19. Cho J, Wang CM, Chan HM, Rickman JM, Harmer MP (2002) *J Mater Sci* 37:59. doi:10.1023/A:1013185506017
20. Dillon SJ, Tang M, Carter WC, Harmer MP (2007) *Acta Mater* 55:6208
21. Dillon SJ, Harmer MP (2007) *Acta Mater* 55:5247
22. Dillon SJ, Harmer MP (2008) *J Eur Ceram Soc* 28:1485
23. Baram M, Kaplan WD (2006) *J Mater Sci* 41:7775. doi:10.1007/s10853-006-0897-7
24. Sadan H, Kaplan WD (2006) *J Mater Sci* 41:5099. doi:10.1007/s10853-006-0437-5
25. Levi G, Kaplan WD (2006) *J Mater Sci* 41:817. doi:10.1007/s10853-006-6565-0
26. Straumal BB, Mazilkin AA, Kogtenkova OA et al (2007) *Philos Mag Lett* 87:423
27. Straumal B, Valiev R, Kogtenkova O et al (2008) *Acta Mater* 56:6123
28. Divinski SV, Lohmann M, Herzog Chr et al (2005) *Phys Rev B* 71:104104
29. Chang L-S, Rabkin E, Straumal BB et al (1999) *Acta Mater* 47:4041
30. Straumal BB, Polyakov SA, Chang L-S et al (2007) *Int J Mater Res* 98:451
31. Straumal B, Prokofjev SI, Chang L-S et al (2001) *Def Diff Forum* 194:1343
32. Rabkin EI, Semenov VN, Shvindlerman LS et al (1991) *Acta Metall Mater* 39:627
33. Noskovich OI, Rabkin EI, Semenov VN et al (1991) *Acta Metall Mater* 39:3091
34. Straumal BB, Noskovich OI, Semenov VN et al (1992) *Acta Metall Mater* 40:795

35. Straumal B, Rabkin E, Lojkowski W et al (1997) *Acta Mater* 45:1931
36. Gupta VK, Yoon DH, Meyer HM et al (2007) *Acta Mater* 55:3131
37. Luo J, Gupta VK, Yoon DH et al (2005) *Appl Phys Lett* 87:231902
38. Molodov DA, Czubyko U, Gottstein G et al (1995) *Philos Mag Lett* 72:361
39. Schölhammer J, Baretzky B, Gust W et al (2001) *Interface Sci* 9:43
40. Straumal B, Sluchanko NE, Gust W (2001) *Def Diff Forum* 188:185
41. Higashi K, Nieh TG, Mabuchi M et al (1995) *Scripta Metall Mater* 32:1079
42. Takayama Y, Tozawa T, Kato H (1999) *Acta Mater* 47:1263
43. Nieh TG, Henshall CA, Wadsworth J (1984) *Scripta Metall* 18:1405
44. Nieh TG, Gilman PS, Wadsworth J (1985) *Scripta Metall* 19:1375
45. Higashi K, Okada Y, Mukai T et al (1991) *Scripta Metall* 25:2053
46. Iwasaki H, Mori T, Mabuchi M et al (1998) *Acta Mater* 46:6351
47. Mabuchi M, Higashi K, Imai T (1991) *Scripta Metall* 25:1675